Journal of Physics: Conference Series

PAPER • OPEN ACCESS

BNCT dosimetry: peculiarities and methods

View the article online for updates and enhancements.

IOP ebooks™

Bringing you innovative digital publishing with leading voices to create your essential collection of books in STEM research.

Start exploring the collection - download the first chapter of every title for free.

BNCT dosimetry: peculiarities and methods

G Gambarini[1,2,3], D Bettega[2,3], A Gebbia[2], E Artuso[2], M Felisi[2], D Giove[2,3], V Klupak[4], L Viererbl[4] and M Vins[4]

[1]Università degli Studi di Milano, Department of Physics, Milano, Italy.
[2]INFN Istituto Nazionale di Fisica Nucleare, Section of Milan, Milano, Italy
[3]Department of Neutron Physics, Research Centre Řež, Czech Republic

E-mail: grazia.gambarini@mi.infn.it

Abstract. Dosimetry in tissue exposed to the epithermal neutron beams utilized for BNCT is complex, due to the multiplicity of the possible neutron reactions and consequently of the secondary radiation that contains photons, charged particles and recoil nuclei. Owing to the different radiobiological effectiveness of the various components of the absorbed dose, it is necessary to attain the evaluation of each of them. In addition, the spatial distributions of these dose components changes considerably with size and shape of the irradiated volume. Therefore, BNCT dosimetry requires suitably developed calculations and experimental methods. In this work, Monte Carlo simulations in phantoms of different sizes and shapes have been developed. Experimental methods for separating the dose components, mainly based on gel dosimeters and thermoluminescence detectors, have been applied. Moreover, the change in the absorbed dose resulting from the addition of ^{157}Gd was investigated. Both measurements and calculations have been done with the BNCT epithermal beam of the LVR-15 reactor.

1. Introduction

BNCT dosimetry is a challenging task, particularly in the case of irradiations with epithermal neutrons, as required for deep tumor treatments. In tissue, the epithermal neutrons are moderated mainly by the elastic scattering interactions with hydrogen nuclei ^{1}H(n,n')^{1}H and the energy spectrum of BNCT neutron beams is suitably designed in order to get high fluence of thermal neutrons in a volume centered at a depth of about 2 cm. The radiotherapy dose is due to the charged particles generated in the reactions of thermal neutrons with ^{10}B selectively accumulated in the tumor tissue (^{10}B(n,α)^{7}Li), here referred to as D_B. In addition to D_B, it is necessary to take into account the dose from all the secondary radiation generated by neutrons, both in tumor and in healthy tissue. The dose contributions that have to be considered can be divided into three general groups, each characterized by a different spatial distribution: the dose coming from the charged particles generated by thermal neutron reactions with particular isotopes, the gamma dose (D_γ) and the dose due to epithermal- and fast-neutron elastic and anelastic collisions (D_{fast}).

The charged particles have a short range and then a spatial distribution directly related to the distribution of the thermal neutron fluence Φ_{th}, and the absorbed dose can be evaluated, in each position, by means of the corresponding kerma factor. The spatial distribution of Φ_{th} is considerably dependent on both size and shape of the irradiated volume. A significant percentage of the absorbed dose comes from gamma radiation, partially due to background (not considered in this work) and partially to the photons of 2.2 MeV emitted in the reactions of thermal neutrons with hydrogen (^{1}H(n,γ)^{2}H). This emission, in each point of the irradiated volume, is linearly correlated to the thermal

neutron fluence in that point but, owing to the long range in tissue of the 2.2 MeV photons, the resulting dose (D_γ) undergoes changes, due to variations of shape or size of the irradiated volume, greater than those of the thermal neutron fluence.

A lower but significant dose contribution is given by neutrons with E > 0.5 eV, whose fluence is here referred to as Φ_{fast}. The spatial distribution of D_{fast} is not greatly dependent on the geometry of the irradiated volume.

Both D_B and D_γ have spatial distributions significantly dependent on size and shape of the irradiated volume and on the direction of incidence of the neutron beam. In order to estimate the influence of the unavoidable lack of precision of the input data for dose measurements or calculations, for the issues described above, appropriate experimental and computational evaluations have been carried out.

Moreover, a few evaluations on neutron fluence and gamma dose in phantom containing ^{157}Gd have been done, because this isotope has been proposed in place of or in addition to ^{10}B, given the effectiveness of Auger electrons in destroying tumor cells. Owing to the high cross section (255000 b) of the reaction ^{157}Gd(n,γ)^{158}Gd, a considerable reduction of Φ_{th} and a noticeable increase of D_γ are expected.

2. Materials and methods

Experimental measurements for BNCT dosimetry require suitably developed methods, because: (i) it is necessary to separate the various dose components owing to their different radiobiological effectiveness; (ii) it is necessary to determine the spatial distribution of each dose component; (iii) the determinations have to be made for the specific geometry of the irradiated volume and (iv) most standard dosimetry methodologies are not applicable with the high neutron fluence-rate proper of BNCT beams (about 10^9 cm^{-2}s^{-1}). A type of detection modality that has shown to be very advantageous, in particular in the case of BNCT epithermal neutron beams, is the gel dosimetry [1]. In fact, gel dosimeters [2-9] allow to determine the spatial distribution of the absorbed dose and, by means of suitable variation of the isotopic composition, they give the possibility of separating all the various dose contributions [10]. If gel dosimeters are prepared in large volumes, the precision of the dose distributions is scarce, because a change of the isotopic composition causes a change of neutron transport. On the opposite, if gel dosimeters are prepared in layers 3 mm thick or similar, inserted in tissue-equivalent phantoms, the accuracy of the determined dose distributions has proven to be high. In phantoms, dose mapping can be attained by means of thermoluminescence detectors (TLDs), with which it is possible to determine D_γ and Φ_{th}. Activation foils can also be used for Φ_{th} measurements, but very small foils and cadmium covers are necessary to avoid sensible change of neutron transport. Concerning the fast neutron dose, a method based on twin ionization chambers has been proposed.

Monte Carlo calculations are widely developed for BNCT dosimetry, based on phantoms of various shapes: cylindrical, ellipsoidal or anthropomorphic. However, a specific determination would be necessary for each specific case of treatment.

In this work, some results are reported, obtained with Fricke-XO gel dosimeters and TLDs. The standard gel dosimeters are water-equivalent and then the absorbed dose, after exposure to epithermal neutrons, is due to photons and to fast neutrons, mainly recoil-proton dose. If a suitable amount of ^{10}B is added to the gel composition, also the charged particles generated by ^{10}B reactions give a contribution to the absorbed dose. If standard gel dosimeters are prepared with heavy water instead of water, fast neutron contribution comes through recoil-deuterons. With suitably developed methods, images and profiles of the various dose contributions are obtained.

Moreover, many MC calculations concerning neutron spectrum and neutron fluence profiles have been performed, in order to investigate the possible variations due to changes of size or shape of the irradiated volume [11]. The last results are here reported.

3. Results

Several measurements and calculations have been performed with the epithermal neutron beam of the LVR-15 research reactor, designed for BNCT at the Research Centre Řež. Different water phantoms have been experimented: standard ($40x40x20$ cm^3), cubic ($20x20x20$ cm^3) and spherical (diameter 16 cm). MC simulations have been developed to obtain energy spectra, longitudinal or transversal profiles of D_γ, Φ_{th} and Φ_{fast}. Experimental images of D_γ, D_{fast}, D_B and Φ_{th} have been obtained in the standard phantom and in a cylindrical one (14 cm in height, 16 cm in diameter). Considerable variations of Φ_{th} and even more of D_γ were found in the various different phantoms. In Figure 1, some results of MC calculations are reported.
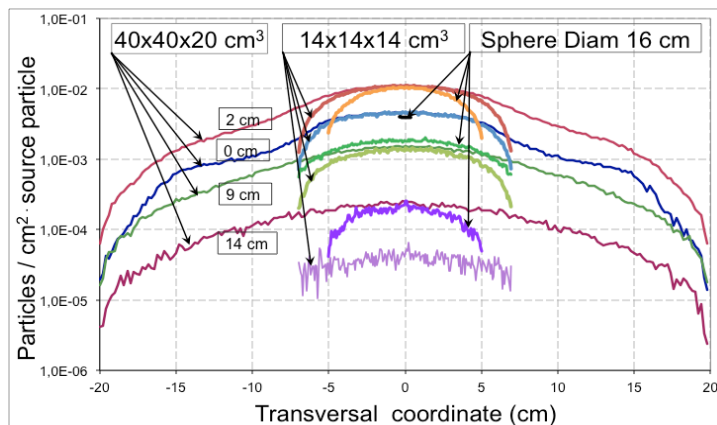
Figure 1. Calculated transversal profiles of thermal neutron fluence in the standard ($40x40x20$ cm^3), cubic ($14x14x14$ cm^3) and spherical ($\varnothing = 16$ cm) phantoms, at depth of 0 cm, 2 cm, 9 cm and 14 cm.

In Figure 2, the calculated profile of Φ_{fast} and the measured profile of D_{fast} are shown and in Figure 3 the ratio D_{fast}/Φ_{fast} is reported. In order to investigate the cause of this difference of the trends vs depth, some considerations about the change of neutron energy-spectrum with increasing depth have been done. In Figure 4, the energy spectra from 0.5 eV onwards, in water at different depths, are reported. The integral of the fluence values in three regions of energy has been evaluated: 10^{-5}-10^{-3} MeV, 10^{-3}-10^{-1} MeV and 10^{-1}-10 MeV. In Figure 5, the results for the various depths are reported. It is evident that, with increasing depth, the relative contribution of the lower energies decreases and that of the higher energies increases. This result is consistent with the increase of the ratio D_{fast}/Φ_{fast} with increasing the depth in water.

Some results showing the great increase of D_γ in presence of 100 µg/g of ^{157}Gd are reported in Figure 6 (Monte Carlo) and Figure 7 (experimental). The experimental results were attained with gel dosimeters (standard and containing ^{157}Gd) by means of suitable algorithms and with TLDs.
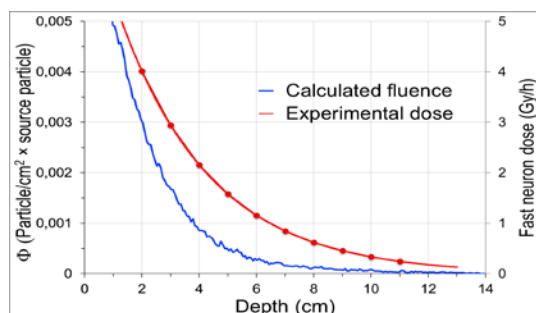

Figure 2. Profiles, along the beam axis, of D_{fast} and of the fluence of neutrons with E > 0.5 eV.
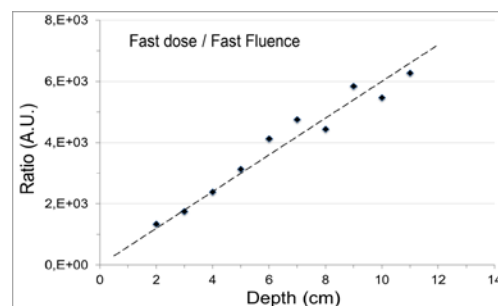

Figure 3. Ratio between the dose and fluence values reported in Figure 2.
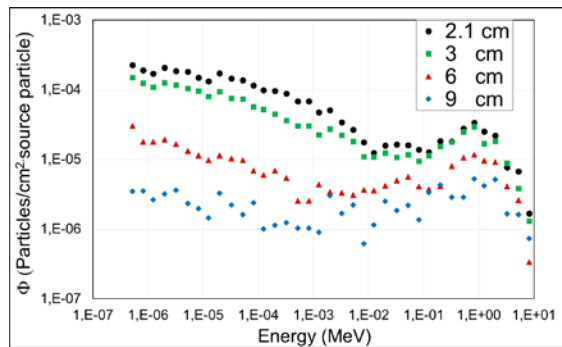
Figure 4. Energy spectra of neutrons with E > 0.5 eV at depths in water of 2.1, 3, 6 and 9 cm.
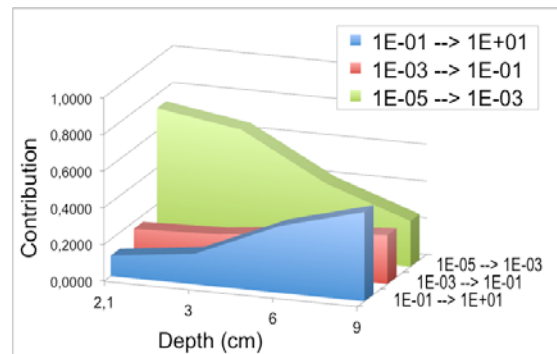

Figure 5. Integral neutron fluence in three regions of energy, vs depth in water.
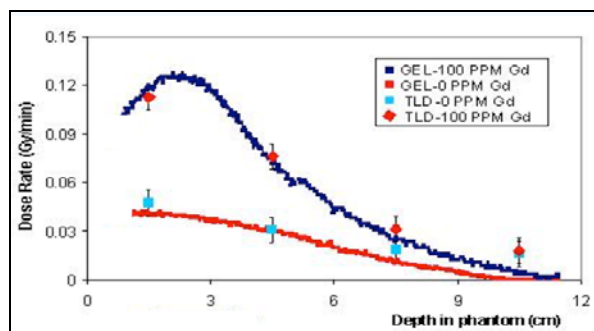

Figure 6. Measured **g**amma dose in a cylindrical phantom of water containing *100* µg/g of ^{157}Gd and of water without ^{157}Gd.
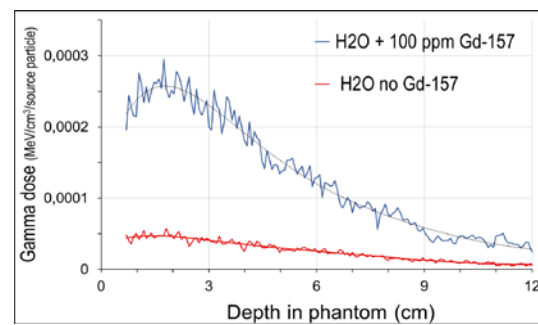

Figure 7. Calculated gamma dose in a cubic phantom of water containing *100* µg/g of ^{157}Gd and of water without ^{157}Gd.

4. Conclusions

The outcomes obtained with the various detectors were mutually consistent and complementary. The results of the work can give useful information on the topic. In particular, they allow a first estimate of the extent of the changes that may occur by changing the shape or size of the irradiated volumes.

5. References

[1] Khajeali A *et al* 2015 *Appl. Radiat. Isot.* **103** 72
[2] Hill B *et al* 2002 *Phys. Med. Biol.* **47** 4233-46
[3] Healy B J *et al* 2003 *Med. Phys.* **30** 2282-91
[4] Mather M L *et al* 2003 *Phys. Med. Biol.* **48** N269-75
[5] Hill B *et al* 2005 *Med. Phys.* **32** 1589-97
[6] Venning A *et al* 2005 *Nucl. Instrum. Meth. A* **555** 396-402
[7] Hurley C *et al* 2006 *Nucl. Instrum. Meth. A* **565** 801-11
[8] Baldock C 2009 *J. Phys.: Conf. Ser.* **164** 012002
[9] Gorjiara T *et al* 2011 *Phys. Med. Biol.* **56** 4685-99
[10] Gambarini G *et al* 2015 *Radiat. Phys. Chem.* **116** 21
[11] Gambarini G *et al* ASTM, STP160 (in press)